

Spin Frustration and Orbital Order in Vanadium Spinels

Yukitoshi MOTOME^{1*} and Hirokazu TSUNETSUGU²

¹*RIKEN (The Institute of Physical and Chemical Research), Saitama 351-0198, Japan*

²*Yukawa Institute for Theoretical Physics, Kyoto University, Kyoto 606-8502, Japan*

We present the results of our theoretical study on the effects of geometrical frustration and the interplay between spin and orbital degrees of freedom in vanadium spinel oxides AV_2O_4 ($A = \text{Zn, Mg or Cd}$). Introducing an effective spin-orbital-lattice coupled model in the strong correlation limit and performing Monte Carlo simulation for the model, we propose a reduced spin Hamiltonian in the orbital ordered phase to capture the stabilization mechanism of the antiferromagnetic order. Orbital order drastically reduces spin frustration by introducing spatial anisotropy in the spin exchange interactions, and the reduced spin model can be regarded as weakly-coupled one-dimensional antiferromagnetic chains. The critical exponent estimated by finite-size scaling analysis shows that the magnetic transition belongs to the three-dimensional Heisenberg universality class. Frustration remaining in the mean-field level is reduced by thermal fluctuations to stabilize a collinear ordering.

KEYWORDS: vanadium spinel oxides, pyrochlore lattice, geometrical frustration, t_{2g} electrons, Kugel-Khomskii model, orbital ordering, antiferromagnetic ordering, Heisenberg universality class, thermal fluctuation, order-by-disorder mechanism

1. Introduction

Spinels are one of the most typical geometrically-frustrated systems. Among them, the so-called B spinel oxides AB_2O_4 , where A cations are nonmagnetic, have attracted much interests since magnetic B cations form the pyrochlore lattice, which consists of a three-dimensional (3D) network of corner-sharing tetrahedra. The system suffers from strong magnetic frustration: Magnetic correlations are strongly suppressed and complex phenomena may appear at low temperatures due to a large number of nearly-degenerate ground states.

In this paper, we will investigate typical B spinels AV_2O_4 with divalent nonmagnetic A cations such as Zn, Mg or Cd. Besides the geometrical frustration, these vanadium spinels have another key issue, the orbital degree of freedom. Since each V^{3+} cation has two $3d$ electrons in threefold t_{2g} levels, the system has the orbital degree of freedom in addition to the spin. Hence, vanadium spinel oxides are intriguing systems which provide two important issues in strongly correlated systems, i.e., geometrical frustration and the interplay between spin and orbital degrees of freedom.

Vanadium spinels AV_2O_4 ($A = \text{Zn, Mg or Cd}$) show two different phase transitions at low temperatures; one occurs at around 50K and the other is at around 40K.¹ Note that the transition temperatures are significantly lower than Curie-Weiss temperature $\sim 1000\text{K}$,² which is attributed to the effect of geometrical frustration. The former is a structural transition from high-temperature cubic phase to low-temperature tetragonal phase. The latter is a magnetic transition with a collinear antiferromagnetic (AFM) ordering. The magnetic structure consists of the staggered ordering with $\uparrow\downarrow\uparrow\downarrow\cdots$ structure along the xy chains and the period-four ordering with $\uparrow\uparrow\downarrow\downarrow\cdots$ structure along the yz and zx chains³ [see

Fig. 1 (b)]. (We take the z axis in the tetragonal c direction.) The issue is the microscopic mechanism of the two transitions: How is the degeneracy due to the geometrical frustration lifted? What is the role of the orbital degree of freedom?

The authors have proposed an effective spin-orbital-lattice model for this problem and shown that the two transitions are well reproduced by Monte Carlo (MC) simulation performed for this model.^{5,6} In the present study, we will focus on the magnetic frustration in the spin-orbital coupled system. We will introduce a reduced spin model to explain the low energy physics in the orbital ordered phase, and clarify the nature of the magnetic transition including its critical properties.

This paper is organized as follows. In Sec. 2, we introduce the effective spin-orbital-lattice model which has been derived in the previous publications,^{5,6} and describe the method of calculations. In Sec. 3, we propose a reduced spin Hamiltonian in the orbital ordered phase and explain the microscopic mechanism of stabilizing the complex AFM ordering. Numerical analysis of the critical exponent is also shown. Section 4 is devoted to summary.

2. Model and Method

We start from a multiorbital Hubbard model with three t_{2g} orbitals on the pyrochlore lattice, and consider the perturbation in the strong correlation limit to describe the low energy physics of the insulating vanadium spinels. By using atomic eigenstates with two $3d$ electrons per site in a high-spin state as the unperturbed states, we derive the effective spin-orbital-lattice coupled model (the so-called Kugel-Khomskii type Hamiltonian⁴) in the form^{5,6}

$$H = H_{\text{so}} + H_{\text{JT}}, \quad (1)$$

$$H_{\text{so}} = -J \sum_{\langle ij \rangle} h_{ij} - J_3 \sum_{\langle\langle ij \rangle\rangle} h_{ij}, \quad (2)$$

*E-mail: motome@riken.jp

$$h_{ij} = (A + B\mathbf{S}_i \cdot \mathbf{S}_j)[n_{i\alpha(ij)}\bar{n}_{j\alpha(ij)} + \bar{n}_{i\alpha(ij)}n_{j\alpha(ij)}] + C(1 - \mathbf{S}_i \cdot \mathbf{S}_j)n_{i\alpha(ij)}n_{j\alpha(ij)}, \quad (3)$$

$$H_{\text{JT}} = \gamma \sum_i Q_i \epsilon_i + \sum_i Q_i^2/2 - \lambda \sum_{\langle ij \rangle} Q_i Q_j, \quad (4)$$

where \mathbf{S}_i is the $S = 1$ spin operator and $n_{i\alpha}$ is the density operator for site i and orbital $\alpha = 1$ (d_{yz}), 2 (d_{zx}), 3 (d_{xy}). Here, $\bar{n}_{i\alpha} = 1 - n_{i\alpha}$ and we impose a local constraint $\sum_{\alpha=1}^3 n_{i\alpha} = 2$ at each site. The summations with $\langle ij \rangle$ and $\langle\langle ij \rangle\rangle$ are taken over the nearest-neighbor (NN) sites and third-neighbor sites, respectively. Here, we take into account only the dominant σ -bond hopping integrals in the original multiorbital Hubbard model, for instance, hoppings between d_{xy} orbitals in the same xy plane.^{5,6} This approximation results in the orbital diagonal interaction in H_{so} ; $\alpha(ij)$ is the orbital which gives rise to the σ bond between sites i and j . H_{JT} describes the orbital-lattice coupling part, where γ is the electron-phonon coupling constant of the tetragonal Jahn-Teller (JT) mode, Q_i denotes the amplitude of local lattice distortion at site i , and $\epsilon_i = n_{i1} + n_{i2} - 2n_{i3}$. λ describes the interaction between NN JT distortions, which mimics the cooperative aspect of the JT distortion.

An important feature of the model (1) is the symmetry of the intersite interactions. In the spin part, the interaction is isotropic Heisenberg type. On the other hand, in the orbital part, it depends only on the density operator, that is, there is no transverse component which mixes different orbitals. Hence, the orbital interaction is three-state Potts type corresponding to three t_{2g} states. Moreover, it depends on bond direction and also orbital states at both ends of a bond. These peculiar properties of the orbital interactions are crucial to trigger the orbital ordering by lifting the degeneracy in the present frustrated system.^{5,6}

The parameters in H_{so} are given by the coupling constants in the starting multiorbital Hubbard Hamiltonian, and in the following we use the reasonable estimates given in Ref. 6 as $J_3/J = 0.02$ with $J \simeq 200\text{K}$, $A = 1.21$, $B = 0.105$, and $C = 0.931$. For the JT parameters, we take $\gamma^2/J = 0.04$ and $\lambda/J = 0.15$, which are typical values to have the tetragonal distortion consistent with the experimental result.⁶ Hereafter, we will set the lattice constant of the cubic unit cell as a length unit and use the convention of the Boltzmann constant $k_B = 1$.

We have studied thermodynamic properties of the model (1) by employing classical Monte Carlo (MC) simulation to avoid the negative sign problem due to the geometrical frustration of the pyrochlore lattice. Since quantum nature exists only in the spin $S = 1$ operators in H_{so} , we approximate them by classical vectors with unit modulus.⁶ We typically perform 10^5 MC samplings for measurements after 10^5 steps for thermalization. System sizes are up to $L^3 = 12^3$ in the cubic units, which includes $12^3 \times 16$ vanadium sites.

3. Results

3.1 Reduced spin model under orbital ordering

MC results show that as temperature decreases, first an orbital ordering takes place with the tetragonal JT

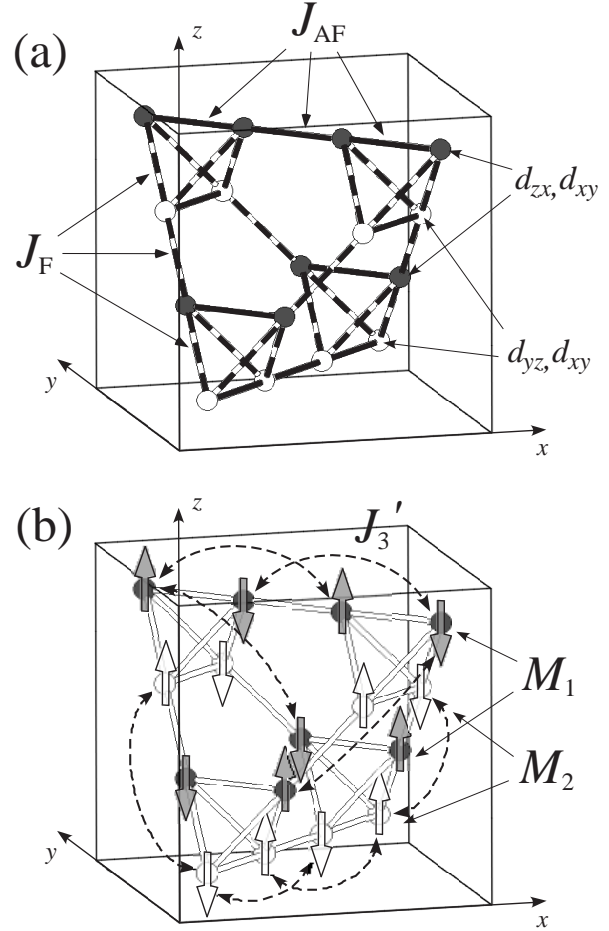


Fig. 1. (a) Effective spin exchange interactions for nearest neighbors in the orbital ordered phase in a cubic unit cell of the pyrochlore lattice. White (gray) circles are the V sites where the d_{yz} and d_{xy} (d_{zx} and d_{xy}) orbitals are occupied. Solid (dashed) bonds represent the strong AFM interactions J_{AF} (the weak FM interactions J_{F}) in the xy (yz and zx) planes. (b) Effective spin exchange interactions for third neighbors, J'_3 . Two sublattices are shown which are connected by J'_3 .

distortion, corresponding to the structural transition in experiments.⁶ This is triggered by the highly anisotropic nature of the three-state Potts-type orbital interaction described above. This transition is discontinuous, and the orbital moment shows a large jump at the transition temperature $T_O \simeq 0.19J$. The ordering structure is A type, i.e., the layered order with alternative stacking of (d_{zx} , d_{xy}) and (d_{yz} , d_{xy}) occupied planes in the z direction as shown in Fig. 1 (a).

Since the orbital polarization below T_O is large and quickly converges to the saturated value,⁶ it is convenient to consider a reduced spin Hamiltonian by freezing the orbital degree of freedom in order to capture the low energy physics in the orbital ordered phase. The reduced spin Hamiltonian is obtained by replacing the orbital parts in Eq. (2) by their mean values in the fully polarized state. For instance, we replace $n_{i3}n_{j3}$ and $n_{i3}\bar{n}_{j3}$ in H_{so} by $\langle n_{i3}n_{j3} \rangle = 1$ and $\langle n_{i3}\bar{n}_{j3} \rangle = 0$, respectively, for the bonds in the xy planes. Then we end up with the

reduced model in the form

$$H_{\text{spin}} = \sum_{\langle ij \rangle \in xy} J_{\text{AF}} \mathbf{S}_i \cdot \mathbf{S}_j + \sum_{\langle ij \rangle \in yz, zx} J_{\text{F}} \mathbf{S}_i \cdot \mathbf{S}_j + \sum_{\langle\langle ij \rangle\rangle} J'_3 \mathbf{S}_i \cdot \mathbf{S}_j. \quad (5)$$

The first two terms describe the NN spin exchange interactions, in which the former (latter) summation is taken over the NN pairs in the xy (yz and zx) planes. $J_{\text{AF}} = JC > 0$ is antiferromagnetic (AFM) and $J_{\text{F}} = -JB < 0$ is ferromagnetic (FM). These exchange interactions are shown in Fig. 1 (a). The last term describes the third-neighbor interactions, where the summation is taken over the third-neighbor σ bonds shown in Fig. 1 (b). $J'_3 = J_3C > 0$ is AFM. Here we omit the orbital-lattice part for simplicity.

First we consider only the NN exchange interactions. One important point is the magnitude of two different interactions J_{AF} and J_{F} . By using the parameters in Sec. 2, we obtain $J_{\text{AF}} \simeq 0.931J$ and $|J_{\text{F}}| \simeq 0.105J$, and hence the AFM exchange in the xy planes is about ten times stronger than the FM exchange in the yz and zx planes. Thus, the system can be regarded as one-dimensional (1D) AFM chains coupled by weak FM exchange interactions. Another key feature is the frustration due to the interchain coupling J_{F} . Once the AFM correlation develops along the xy chains by the strong J_{AF} , coupling of the xy chains are frustrated; in the mean-field level, the total energy does not depend on the relative angle of AFM moments in any two xy chains. Therefore, the system is reduced to independent 1D AFM chains and it is hard to establish a three-dimensional (3D) AFM order at this stage.

The frustration remaining among the xy chains is almost reduced by the small third-neighbor exchange $J'_3 \simeq 0.0186J$. As shown in Fig. 1 (b), J'_3 connects the parallel xy chains and stabilizes a 3D AFM ordering. Note that however there still remains frustration between two sublattices; one consists of (d_{zx}, d_{xy}) occupied sites and the other consists of (d_{yz}, d_{xy}) occupied sites. The relative angle between two sublattice moments \mathbf{M}_1 and \mathbf{M}_2 is free in the mean-field level. Reduction of the frustration will be discussed in Sec. 3.3.

The picture based on the reduced spin model (5) is confirmed by our MC calculations. Figure 2 shows the temperature dependences of the NN and third-neighbor spin correlations in the effective spin-orbital-lattice model (1): $S_{\text{NN}(3\text{rd})}^{(\nu)} = \sum_{\langle ij \rangle (\langle\langle ij \rangle\rangle) \in \nu} \langle \mathbf{S}_i \cdot \mathbf{S}_j \rangle / N_{\text{b}}$, where N_{b} is the number of bonds in the summation and $\nu = xy, yz, zx$. Note that $S^{(yz)}$ equals to $S^{(zx)}$ by symmetry. Below the orbital ordering temperature T_{O} , AFM correlations develop along the xy chains ($S_{\text{NN}}^{(xy)} < 0$ and $S_{3\text{rd}}^{(xy)} > 0$), while correlations in the yz and zx chains remain small. Particularly, the NN correlations $S_{\text{NN}}^{(yz)}$ become almost zero because of the frustration in the interchain coupling J_{F} . Below $T_{\text{N}} \simeq 0.12J$ (which will be assigned to the 3D AFM transition temperature in Sec. 3.2), $S_{3\text{rd}}^{(xy)}$ rapidly grows due to J'_3 . Thus the system becomes highly one-dimensional below T_{O} , and 3D interchain correlations develop below T_{N} .

Consequently, the orbital ordering introduces the spatial anisotropy in the intersite spin exchange interactions,

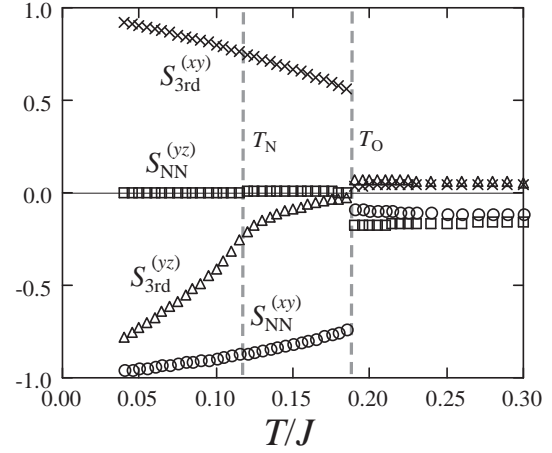


Fig. 2. Temperature dependences of spin correlations for the system size $L = 12$. Error bars are smaller than the symbol sizes. See the text for details.

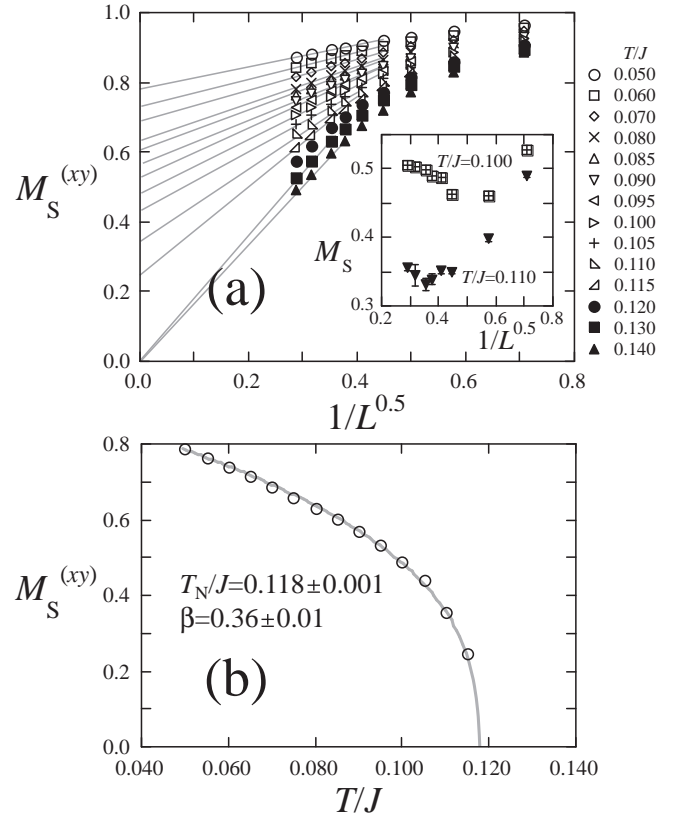


Fig. 3. (a) System size extrapolation of the staggered moment along the xy chains. Lines are the linear fits for the data. Inset: System size dependence of M_{S} . (b) Temperature dependence of the extrapolated data in (a). The curve shows the fit by $M_{\text{S}}^{(xy)} \propto (T_{\text{N}} - T)^{\beta}$. Error bars are smaller than the symbol sizes.

which plays a key role to reduce the geometrical frustration. The system is effectively reduced to weakly-coupled 1D chains and finds a way to establish a 3D AFM order.

3.2 Magnetic transition and universality class

The 3D AFM order is indeed found to occur in our MC results for the model (1). The staggered magnetic

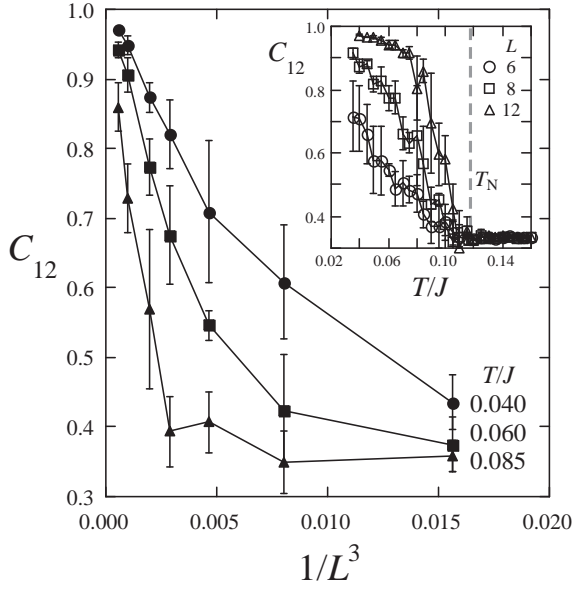


Fig. 4. (a) Temperature dependence of the collinearity. (b) System size dependence. The lines are guides for the eyes.

moment M_S , which is the magnitude of the staggered moment \mathbf{M}_1 or \mathbf{M}_2 , grows continuously at $T \sim 0.12J < T_O$. To determine the transition temperature T_N precisely, we perform a finite-size scaling analysis. As shown in the inset of Fig. 3 (a), M_S shows non-monotonic size dependence within the range of the system sizes calculated here, probably because of the large spatial anisotropy of the AFM correlations discussed in Sec. 3.1. Instead, we use the staggered moment along the AFM xy chains, $M_S^{(xy)}$, which is defined by the average of the magnitude of AFM moments in the xy chains.⁶ The restricted summation reduces effects of anisotropic correlations.

Fig. 3 (a) shows the system-size dependences of $M_S^{(xy)}$. The MC data are fitted by a linear function of $1/\sqrt{L}$ (Ref. 6). The values extrapolated to $L \rightarrow \infty$ are plotted as a function of temperature in Fig. 3 (b).

The transition temperature T_N and the critical exponent β are obtained by the scaling fit $M_S^{(xy)} \propto (T_N - T)^\beta$ for the data in Fig. 3 (b). The best fit gives the estimates $T_N/J = 0.118 \pm 0.001$ and $\beta = 0.36 \pm 0.01$. The exponent β is consistent with that of the 3D isotropic Heisenberg model with short-range interactions, $\beta = 0.365$ (Ref. 7), which indicates that the AFM transition in the present system belongs to the 3D Heisenberg universality class.

3.3 Collinear ordering due to ‘order by disorder’

As explained in Sec. 3.1, in the mean-field level, frustration remains between two sublattice moments \mathbf{M}_1 and \mathbf{M}_2 shown in Fig. 1 (b) even when 3D long-range order is well established in each sublattice. Note that either M_S or $M_S^{(xy)}$ in Sec. 3.2 does not give information about the relative angle between \mathbf{M}_1 and \mathbf{M}_2 .

Here, we measure the collinearity by $C_{12} = \langle \cos^2 \theta_{12} \rangle$,

where θ_{12} describes the angle between \mathbf{M}_1 and \mathbf{M}_2 . Figure 4 shows our MC results of C_{12} for the model (1). C_{12} rapidly increases below T_N as shown in the inset. System-size dependences of C_{12} show that the data approach 1 in the thermodynamic limit below T_N , which indicates that the magnetic order is collinear.

The collinear ordering is understood by the so-called order-by-disorder mechanism.⁸ Our MC results show that the frustration remaining in the mean-field level is reduced by thermal fluctuations and the collinear AFM state is stabilized. In Ref. 5, the authors have shown that quantum fluctuations also favor the collinear state to minimize the zero point energy of magnons. It is well known that both thermal and quantum fluctuations favor a collinear state in many frustrated spin systems. This is also the case in the present system.

The magnetic structure obtained by MC calculations is shown in Fig. 1 (b). The ordering pattern is consistent with the experimental result by the neutron scattering.³

4. Summary

We have found that the interplay between spin and orbital is crucial in the geometrically-frustrated vanadium spinels. The orbital ordering introduces spatial anisotropy in the effective spin exchange interactions and drastically reduces the magnetic frustration. In the orbital ordered phase, the system can be regarded as weakly coupled 1D AFM chains. By applying the finite-size scaling analysis to numerical data, we have shown that the AFM transition belongs to the universality class of the 3D unfrustrated Heisenberg model. We have also pointed out the importance of thermal fluctuations to stabilize the collinear AFM state by the order-by-disorder mechanism.

Acknowledgment

This work was supported by a Grant-in-Aid and NAREGI from the Ministry of Education, Science, Sports, and Culture. A part of the work was accomplished during Y. M. was staying at the Yukawa Institute of Theoretical Physics, Kyoto University, with the support from The 21st Century for Center of Excellence program, ‘Center for Diversity and Universality in Physics’.

- 1) Y. Ueda, N. Fujiwara and H. Yasuoka: J. Phys. Soc. Jpn. **66** (1997) 778.
- 2) Muhtar, F. Takagi, K. Kawakami and N. Tsuda: J. Phys. Soc. Jpn. **57** (1988) 3119.
- 3) S. Niziol: Phys. Status Solidi A **18** (1973) K11.
- 4) K.I. Kugel and D.I. Khomskii, Zh. Eksp. Teor. Fiz. **64** (1973) 1429 [Sov. Phys. JETP **37** (1973) 725].
- 5) H. Tsunetsugu and Y. Motome: Phys. Rev. B **68** (2003) 060405(R).
- 6) Y. Motome and H. Tsunetsugu: preprint (cond-mat/0406039), to be published in Phys. Rev. B.
- 7) J.C. Le Guillou and J. Zinn-Justin: Phys. Rev. Lett. **39** (1977) 95.
- 8) J. Villain: J. Phys. C: Solid State Phys **10** (1977) 1717.